ACS APPLIED MATERIALS & INTERFACES

Research Article

www.acsami.org

Superior Antibacterial Activity of Zinc Oxide/Graphene Oxide Composites Originating from High Zinc Concentration Localized around Bacteria

Yan-Wen Wang,[†] Aoneng Cao,[†] Yu Jiang,[†] Xin Zhang,[†] Jia-Hui Liu,[‡] Yuanfang Liu,[†,‡] and Haifang Wang*[,†]

[†]Institute of Nanochemistry and Nanobiology, Shanghai University, Shanghai 200444, China

[‡]Beijing National Laboratory for Molecular Sciences, College of Chemistry and Molecular Engineering, Peking University, Beijing 100871, China

Supporting Information

ABSTRACT: New materials with good antibacterial activity and less toxicity to other species attract numerous research interest. Taking advantage of zinc oxide (ZnO) and graphene oxide (GO), the ZnO/GO composites were prepared by a facile one-pot reaction to achieve superior antibacterial properties without damaging other species. In the composites, ZnO nanoparticles (NPs), with a size of about 4 nm, homogeneously anchored onto GO sheets. The typical bacterium *Escherichia coli* and HeLa cell were used to evaluate the antibacterial activity and cytotoxicity of the ZnO/GO composites, respectively. The synergistic effects of GO and ZnO NPs led to the superior antibacterial activity of the composites. GO helped the dispersion of ZnO NPs, slowed the dissolution of ZnO, acted as the storage site for the dissolved zinc ions, and enabled the intimate contact of *E. coli* with ZnO NPs and zinc ions as well. The close contact enhanced the local zinc concentration pitting on the bacterial membrane and the permeability of the bacterial membrane and thus induced bacterial death. In addition, the ZnO/GO composites were found to be much less toxic to HeLa cells, compared to the equivalent concentration of ZnO NPs in the composites. The results indicate that the ZnO/GO composites are promising disinfection materials to be used in surface coatings on various substrates to effectively inhibit bacterial growth, propagation, and survival in medical devices.

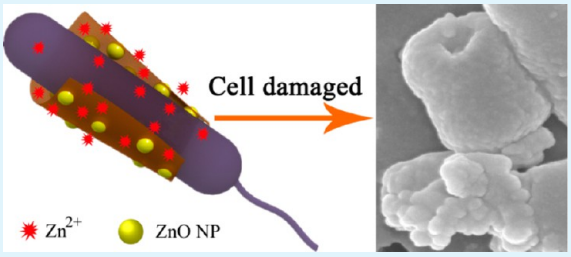

KEYWORDS: *ZnO, graphene oxide, nanocomposite, antibacterial activity, E. coli, cytotoxicity*

INTRODUCTION

Zinc oxide (ZnO) has the inherent advantage of broad antibacterial activities against bacteria,[1,2] fungus,[3,4] and virus.[5] ZnO is listed as a generally recognized safe material by the Food and Drug Administration of the United States (21CFR182.8991).[6] Thus, ZnO has been widely used as an antibacterial agent. In recent years, ZnO nanoparticles (NPs) have been found to show much better antibacterial ability than the counterpart microsized ZnO particles.[1] Release of zinc ions from ZnO was suggested as one of the primary antibacterial mechanisms of ZnO NPs.[7] Moreover, the penetration and disorganization of a bacterial membrane upon contact with ZnO particles also contributed to the antibacterial ability of ZnO NPs.[8,9] However, the easy aggregation of ZnO NPs hampers their antibacterial activity.[10] In addition, at effective antibacterial concentrations, ZnO NPs have also been found to be toxic to eukaryotic cells,[11] plants,[12] and animals.[13] At present, developing ZnO NPs with excellent antibacterial properties and less toxicity to other species is still an attractive challenge.

Graphene oxide (GO) is an oxidized derivative of graphene, a fascinating carbon material that has spurred significant interest in the last 10 years. GO contains a large number of oxygen bonds, such as hydroxyl and epoxy functional groups on the hexagonal network of carbon atoms and carboxyl groups at the edges.[14] These abundant oxygen functional groups not only assist the dispersion of GO in water as a stable colloidal suspension but also provide active sites for functionalization and hybridization with other materials, especially metal and metal oxide through both electrostatic and coordinate approaches.[15] Various metal/metal oxide and GO composites have been synthesized and applied in different fields, such as biosensors, capacitors, and photocatalysts.[16−18] Recently, the antibacterial properties of GO have been reported also.[19−21] GO shows obvious antibacterial activity at concentrations of around 40 μg mL^{-1}. In the meantime, GO possesses good biocompatibility.[22] Therefore, we aim to elucidate that the composite of ZnO NPs and GO may reach more superior antibacterial ability compared to ZnO NPs or GO alone.

Received: November 24, 2013
Accepted: February 4, 2014
Published: February 4, 2014

   dx.doi.org/10.1021/am4053317 | *ACS Appl. Mater. Interfaces* 2014, 6, 2791−2798

Scheme 1. Schematic Illustration of the Synthetic Procedure for the ZnO/GO Composite from the GO Sheet

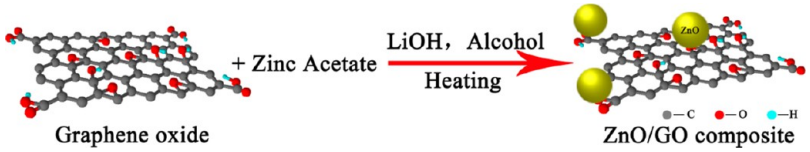

Herein, employing a facile one-pot reaction, we synthesized ZnO/GO composites. A typical bacterium, *Escherichia coli*, was used to evaluate the antibacterial activity and HeLa cells for the cytotoxicity study. The results showed that the composites have a much stronger ability to kill bacteria at low concentrations, which do not affect the viability of the HeLa cells at all. The antibacterial mechanism of the ZnO/GO composites was proposed, and the possible applications were discussed.

RESULTS AND DISCUSSION

Synthesis and Characterization of the ZnO/GO Composites. GO sheets are graphene basal planes covered mostly with epoxy and hydroxyl groups, while carbonyl and carboxyl groups are located at the edges.[14] These oxygen-containing groups, acting as anchor sites, enable the in situ formation of nanostructures on the surfaces and edges of the GO sheets. In this work, we modified the synthesis process of the ZnO/GO composite reported in the previous study[23] to accomplish synthesis in one step, as depicted in Scheme 1. In the reaction, zinc ions from reactant zinc acetate bound to oxygen atoms of negatively charged oxygen-containing functional groups on GO by the electrostatic force and coordination reaction, acting as anchor sites for the growth of ZnO NPs. With the addition of OH^-, a large number of crystal nuclei formed at the anchor sites in a short time. Then, ZnO NPs grew larger along the planes and edges of the GO sheets to form the ZnO/GO composites. Finally, ZnO NPs uniformly anchored on the GO sheets. The density and size of ZnO NPs on GO can be regulated by adjusting the quantity of the reactants (GO and zinc ions) and by altering the reaction time. Two composites were prepared for the following tests: ZnO/GO-1 (mass ratio of ZnO/GO was 3:1) and ZnO/GO-2 (mass ratio of ZnO/GO was 2:1).

Direct evidence of the formation of ZnO/GO composites is given by transmission electron microscopy (TEM) and high-resolution TEM (HRTEM). Parts a and b of Figure 1 show the representative TEM images of ZnO/GO-1 and ZnO/GO-2, respectively. The diameter of ZnO NPs on the GO sheets is around 4 nm according to the HRTEM investigation (Figure 1c). In the HRTEM image of ZnO/GO-1 (Figure 1d), there is a nanocrystal particle on the GO sheet. The distance (0.28 nm) between the adjacent lattice fringes just corresponds to the (100) crystal plane of ZnO (JCPDS no. 36-1415), indicating the existence of ZnO NPs on GO. The structure of the region around the nanocrystal is different from that of the ZnO crystal. The lattice spacing of 0.34 nm corresponds to the graphene structure.[24] The intimate contact between ZnO NPs and graphene indicates the strong interaction of ZnO and GO. The energy-dispersive spectrometry (EDS) spectrum (Figure 1e) of ZnO/GO-1 confirms the presence of zinc and oxygen in the composite.

To further confirm the formation of ZnO/GO composites, the X-ray diffraction (XRD) patterns of ZnO, GO, and the ZnO/GO composites were recorded (Figure 2). Figure 2a is the XRD pattern of GO. A sharp reflection peak at 10.8°

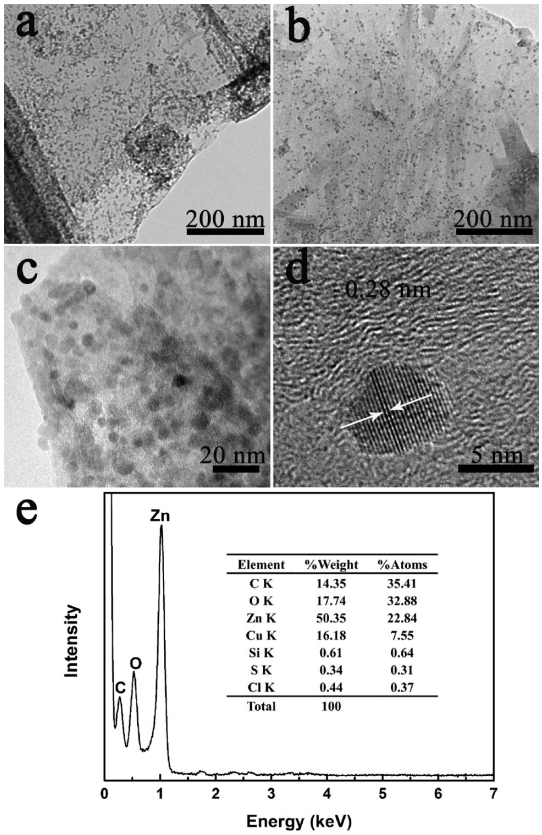

Element	%Weight	%Atoms
C K	14.35	35.41
O K	17.74	32.88
Zn K	50.35	22.84
Cu K	16.18	7.55
Si K	0.61	0.64
S K	0.34	0.31
Cl K	0.44	0.37
Total	100	

Figure 1. TEM characterization of the ZnO/GO composites: (a) ZnO/GO-1; (b) ZnO/GO-2. (c and d) HRTEM images of ZnO/GO-1. (e) EDS spectrum of the ZnO/GO-1 composites, showing the presence of Zn and O.

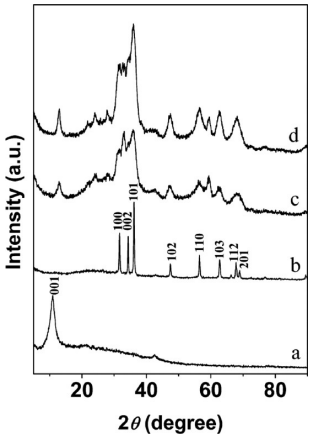

Figure 2. XRD patterns of GO (a), pure bulk ZnO (b), ZnO/GO-2 (c), and ZnO/GO-1 (d).

(Figure 2a), corresponding to the feature diffraction peak (001) of exfoliated GO,[25] is observed. This peak is also observed in the XRD pattern of the ZnO/GO composites (Figure 2c,d),

dx.doi.org/10.1021/am4053317 | ACS Appl. Mater. Interfaces 2014, 6, 2791−2798

although the low content of GO in the composites makes the intensity much lower. In Figure 2c,d, the peaks at 2θ = 31.4°, 35.9°, 47.4°, and 56.3° can be assigned to the (100), (101), (102), and (110) crystalline plane of ZnO (JCPDS no. 36-1415), respectively. The boarder diffraction peaks of the ZnO/GO composites compared with the pure bulk ZnO particles indicate the much smaller size of the ZnO particles on the GO sheets. The size calculated from the Scherrer equation is about 2 nm, which is basically consistent with the size observed in the HRTEM images.

The chemical states of the ZnO/GO composites were detected by X-ray photoelectron spectroscopy (XPS). The representative XPS spectra of C 1s and Zn 2p for ZnO/GO-1 are shown in Figure 3. In the Zn 2p spectrum, two strong peaks

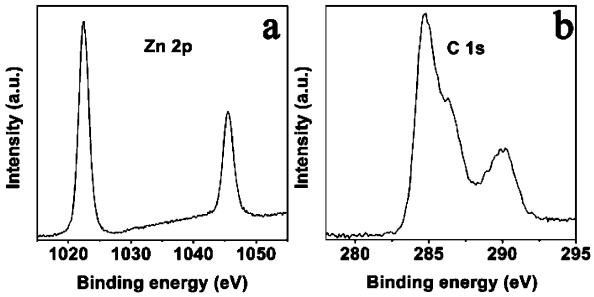

Figure 3. XPS spectra of ZnO/GO-1: (a) Zn 2p; (b) C 1s.

at 1022.4 and 1045.5 eV correspond to the binding energies of Zn $2p_{3/2}$ and Zn $2p_{1/2}$, respectively. The peaks are in agreement with those of pure ZnO,[26] suggesting that zinc in the composites exists in its oxidized state. The C 1s XPS spectrum (Figure 3b) shows two main peaks at 284.6 and 289.9 eV, which could be assigned to the C═C bond (sp^2) of graphene and the existence of O−C═O bonds.[27]

Antibacterial Activity of the ZnO/GO Composites. The antibacterial activity of the ZnO/GO composites was first investigated qualitatively by the disk diffusion assay (Figure 4).

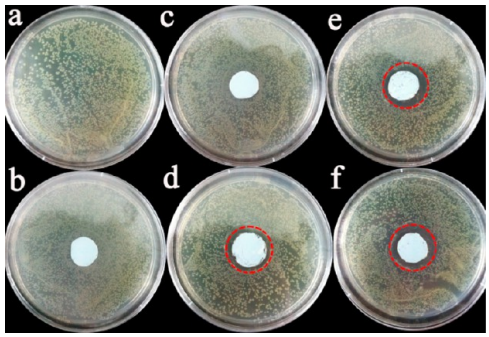

Figure 4. Photographs of the inhibition zone by the disk diffusion assay: (a) control; (b) GO; (c) 1 μg of ZnO/GO-2; (d) 2 μg of ZnO/GO-2; (e) 2 μg of ZnO/GO-1; (f) 4 μg of ZnO/GO-1.

Two composites with different quantities were tested in order to investigate both the concentration and composite component effects on the antibacterial activities. We did not find the inhibition zone in the GO-treated sample (Figure 4b), compared to the control group, which is in the absence of GO and the ZnO/GO composites (Figure 4a). This might be due to the fact that the GO sheets were at low concentration and difficult to diffuse into the agar gel. However, after the addition of the ZnO/GO composites, the inhibition zones are obviously visible. As the quantity of the ZnO/GO composites and the content of ZnO on the GO sheets increase, the inhibitions are more remarkable (parts c and d and parts e and f of Figure 4). The diameter of the inhibition zone of *E. coli* treated with ZnO/GO-1 is a little bit larger than that treated with ZnO/GO-2 under the same conditions (Figure 4d,e). Therefore, the ZnO/GO composites exhibit a concentration- and composite-dependent bactericidal activity.

To further investigate the antibacterial effect of the ZnO/GO composites quantitatively, the growth curves of *E. coli* treated with the composites were measured (Figure 5). The results are

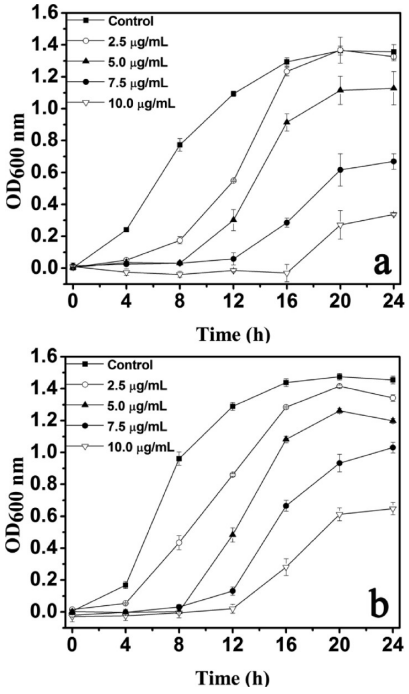

Figure 5. Growth curves of *E. coli*: (a) ZnO/GO-1; (b) ZnO/GO-2.

consistent with qualitative analysis. The reported effective concentration of ZnO NPs is in the range of 0.3−0.6 mg mL^{-1} (depending on the bacterial strain).[28] In this study, the effective concentration of the ZnO/GO composites (2.5 μg mL^{-1}) is very low, in which the concentration of ZnO NPs is only 1.9 μg mL^{-1} for ZnO/GO-1 and 1.7 μg mL^{-1} for ZnO/GO-2. In addition, Li et al.[29] reported that only when the concentration of ZnO NPs increased to 500 μg mL^{-1}, the number of *E. coli* hardly increased within 12 h. In this study, the same inhibition could be achieved with 10 μg mL^{-1} of the ZnO/GO composites. These demonstrate that the ZnO/GO composites possess much stronger antibacterial ability compared to naked ZnO NPs.

Along with the increase of the concentration of the ZnO/GO composites, the growth of *E. coli* is inhibited more and more severely. A noticeable difference in the growth rate between the two composites is observed after 2 h of incubation with the ZnO/GO composites (Figure 5). For ZnO/GO-1, the growth time of the bacteria is delayed by approximately 12 and 16 h at concentrations of 7.5 and 10.0 μg mL^{-1}, respectively, whereas it is 8 and 12 h for ZnO/GO-2 under the same conditions. The results indicate that the inhibitory efficiency of the ZnO/GO composites is primarily dependent on its concentration and the

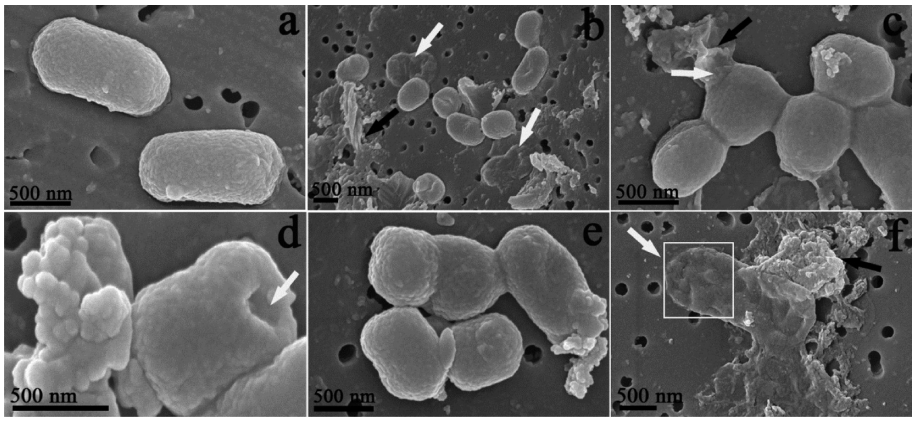

Figure 6. SEM images of *E. coli*: (a) control; (b–d) *E. coli* treated with ZnO/GO-1 for 24 h; (e and f) *E. coli* treated with ZnO/GO-2 for 24 h. White arrows: broken *E. coli*. Black arrows: the ZnO/GO composites. White square: cytoplasm leakage.

content of ZnO in the composites. Overall, the synthesized ZnO/GO composites can be effectively used to kill the bacteria.

Morphology Change of Bacteria after Exposure to the ZnO/GO Composites. The ZnO/GO composites effectively inhibited the growth of *E. coli*. We therefore investigated the morphology changes of *E. coli* cells before and after exposure to the ZnO/GO composites by using scanning electron microscopy (SEM). The untreated *E. coli* cells have rodlike shape and intact surfaces (Figure 6a). After exposure to ZnO/GO-1 for 24 h, the morphology of bacteria significantly changes and a portion of the bacteria is decomposed (Figure 6b,c, white arrows). Most of the bacteria change from rod shape to globular shape with a damaged membrane (Figure 6b–d, white arrows), and the cytoplasm of some bacteria leaks off thoroughly (Figure 6b, white arrows), indicating both outer and inner membrane damage. Similar phenomena also can be seen in bacteria treated with ZnO/GO-2 (Figure 6e,f). In Figure 6f, it is observed that the bacterium is covered by the ZnO/GO composites (black arrows). The membrane of the bacterium apparently collapses, and the cytoplasm has leaked out (white square). SEM investigation indicates that the ZnO/GO composites changed the morphology of *E. coli*, which might eventually induce growth inhibition and bacterial death. To further confirm the membrane disruption of *E. coli* induced by the ZnO/GO composites, the release of nucleotides from bacteria, an indicator of bacterial membrane integrity, was detected by measuring the absorbance at 260 nm. After exposure to the composites, the leakage of nucleotides from bacteria increased with increasing contact time and content of ZnO NPs in the composites (Figure S1 in the Supporting Information, SI). The results provide further evidence of the damage of the bacterial membrane.

Stoimenov et al.[30] reported that the binding of ZnO NPs to the bacterial surface by electrostatic forces directly killed bacteria. The surface abrasiveness of ZnO NPs was assumed to be responsible for the high antibacterial performance of ZnO NPs by initiating disorganization of the cell membrane.[31] Another study suggested that ZnO damaged the membrane of *E. coli* and then led to the cellular internalization of ZnO.[8] In this study, we observed that the amounts of treated bacteria were wrapped by the ZnO/GO composites. The tight contact of the GO sheets and *E. coli* may enable ZnO NPs on the composites to contact tightly with the membrane of *E. coli*, hence inducing rupture of the contacted bacteria.[1,8] We speculated further that wrapping of the ZnO/GO composites might facilitate the direct contact of ZnO NPs with the cell membrane. Then the accumulation or deposition of ZnO NPs on the *E. coli* surface led to the relatively high local concentration of zinc, which eventually causes cell death. In addition, wrapping of the ZnO/GO composites might prevent the bacteria from nourishing themselves from the culture medium.

Solubilization of ZnO NPs on the ZnO/GO Composites in a Culture Medium. Generally, the antibacterial ability of ZnO NPs is usually ascribed to the released zinc ions from ZnO NPs.[29,32] In order to further clarify the antibacterial mechanism of the composites, solubilization of the ZnO/GO composites in a culture medium was investigated (Figure 7). It is observed that zinc quickly dissolves from the ZnO/GO composites at the beginning. After 2 h, released zinc almost reaches saturation. When the concentration of the composites is 5.0 μg mL^{-1}, 30% of zinc dissolves from ZnO/GO-1 and 33% from ZnO/GO-2 after 24 h of incubation. For ZnO/GO-1, when the

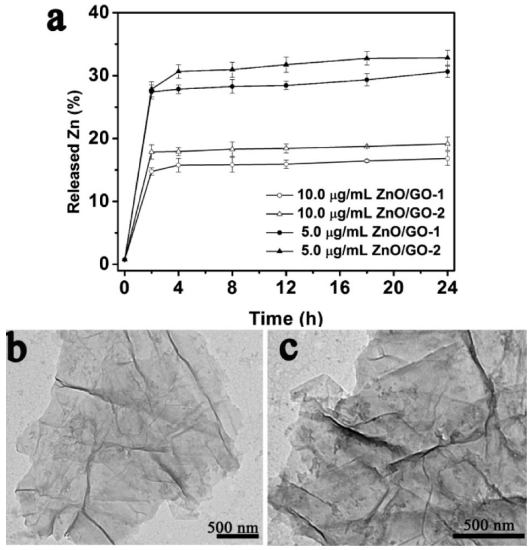

Figure 7. Solubilization of the ZnO/GO composites in a culture medium. (a) Zinc released from the ZnO/GO composites (calculated as the percentage of the released zinc in the total amount of zinc in the composites). (b) TEM image of ZnO/GO-1 after cultured in a medium for 24 h. (c) TEM image of ZnO/GO-2 after cultured in a medium for 24 h.

concentration increases from 5.0 to 10.0 μg mL^{-1}, the dissolution decreases from around 30% to 15%. Although the dissolution percentage changes a lot, the final concentrations of zinc in a culture medium all reach to around 0.9 μg mL^{-1}, no matter what the concentration of the composites is and which composite is tested. The value was not affected by the existence of bacteria in the culture medium (data not shown). The solubility of ZnO NPs in this study is much lower than that in ref 29. It may be due to both the dissolution property of ZnO NPs on GO and the absorption of released zinc on GO. Franklin et al.[32] regarded that solubilization of ZnO was the main reason for the antibacterial ability of ZnO, in which the concentration of zinc ions was found to be around 10 μg mL^{-1}. In our study, however, the concentration of the released zinc was only 0.9 μg mL^{-1}, a concentration that could not damage *E. coli* directly.

We tried to investigate the reasons for the very low solubility of ZnO on the composites, compared to the solubility of ZnO NPs in the previous work (68 μg mL^{-1}).[29] We tested the adsorption of zinc ions on pristine GO when the 60 μg of zinc ions (equivalent quantity of zinc in ZnO/GO-1) and 25 μg of GO (equivalent quantity of GO in ZnO/GO-1) were mixed in 10 mL of a culture medium. It was found that around 21 μg (35%) of zinc ions was adsorbed on GO sheets, while 39 μg (65%) of zinc ions (3.9 μg mL^{-1}) was in the culture medium, much higher than the saturated zinc ion concentration released from GO/ZnO-1 in a culture medium (0.9 μg mL^{-1}). Thus, it is possible that most zinc ions released from ZnO NPs might immediately be absorbed by the GO sheets instead of dispersing into the culture medium. After culturing for 24 h, the ζ potential of GO/ZnO-1 changed from −11.4 to −9.2 mV. The increased ζ potential confirms the adsorption of zinc ions on the composites. The absorbed zinc ions on the GO sheets could directly contact with bacteria, increase the local zinc concentration pitting on the bacterial membrane, and eventually speed up the death of bacteria.

TEM images of the ZnO/GO composites after being cultured with bacteria in the medium for 24 h are shown in Figure 7. Although ZnO NPs become blurry and the number decreases, there are still a number of ZnO NPs anchored on the GO sheets after treatment. In such cases, ZnO NPs on GO may continually dissolve into a culture medium in a slow and sustained mode until Zn NPs are depleted. This might guarantee a long-term antibacterial activity of the ZnO/GO composites.

When the results of the above sections were combined, the released zinc from the composites was much lower than its reported effective concentration and GO alone did not exhibit any antibacterial property in this study. We therefore ascribe the superior antibacterial activity to the synergistic effect of GO and ZnO NPs. Morones et al.[33] reported that only Ag NPs with a diameter of less than 10 nm exhibited direct interaction with a few bacterial strains, including *E. coli*. In this work, GO served as a substrate to deposit well-dispersed and small-sized ZnO NPs, which reduced the aggregation of ZnO NPs and enabled more ZnO to contact with *E. coli* directly. Because of the high absorption capacity of GO for zinc ions, GO also served as the storage site of zinc ions released from ZnO NPs after contact with aqueous media. The intimate contact might increase the local free zinc concentration pitting on the membrane surface of bacteria and thus increase the permeability of the bacterial membrane, which enhanced the exposure of bacteria to zinc. Eventually, the morphology of *E. coli* cells significantly changed and the membranes deformed, wherein some cells died after the cells swelled and the intracellular substances leaked out. Compared to ZnO/GO-2, ZnO/GO-1 contained more ZnO NPs and possessed stronger antibacterial ability because there were more ZnO NPs contacted with the bacterial membrane and higher local free zinc around bacteria in ZnO/GO-1.

Cell Viability Test of the ZnO/GO Composites. To test the toxicity of the composites to other species, HeLa cell was selected. The viability of HeLa cells was assayed after exposure to GO and the ZnO/GO composites by CCK-8 assay (Figures 8 and S2 in the SI), in which the formation of formazan dye

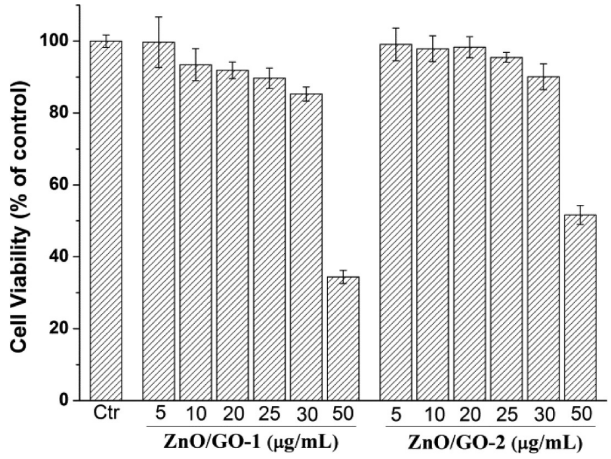

Figure 8. Viability of HeLa cells after expossure to the ZnO/GO composites for 24 h.

indicating the mitochondria activity of cells was tested. The cell viability loss induced by the composites is dose-related. GO exhibited no viability loss, even at relatively high concentrations (50 μg mL^{-1}), indicating the low toxicity of GO to HeLa cells (Figure S2 in the SI). The result is well consistent with the data in our previous work.[22] Similarly, even when the concentration of ZnO/GO-1 reaches 20 μg mL^{-1}, which is 2 times the highest concentration used in the antibacterial experiment in this study, the cell viability is still over 90%. However, a concentration of ZnO NPs (240 μM) identical with that of 20 μg mL^{-1} ZnO/GO-1 decreased the cell viability to 30% (Figure S5 in the SI), which is consistent with our previous report.[34] Obviously, these results illustrate that the ZnO/GO composites cause much lower cytotoxicity than an equivalent amount of ZnO NPs alone. When the concentration of the composites increases to 50 μg mL^{-1}, the viability decreases obviously, especially for ZnO/GO-1 (35%), which contains more ZnO, while the equivalent concentration of ZnO NPs (600 μM) leads to almost total viability loss (8%; Figures 8 and S5 in the SI). Similar to the antibacterial ability of the composites, such a difference in the cytotoxicity might arise from the different contents of ZnO NPs anchored on the surface of the GO sheet. The higher the concentration of ZnO NPs, the more severe the cell damage induced.

The significant different consequences between *E. coli* and HeLa cells might come from the different mechanisms of killing bacteria and killing cells by zinc. For bacteria, the effective contact of bacteria and zinc is necessary, while the uptake of zinc inside cells is essential for cells.[30,31,35,36] Although dissolution of ZnO NPs in cell culture media occurred, the extracellular zinc released from ZnO NPs and zinc on the composites attached to HeLa cells is insufficient to produce

enough bioavailable zinc inside HeLa cells to induce cytotoxicity, even with higher starting concentrations of ZnO NPs.[35,36] More detailed mechanisms need further investigation.

On the whole, the ZnO/GO composite is a promising antibacterial material because the low concentrations of ZnO and GO have no cytotoxicity, but they together present ideal and long-term antibacterial ability.

CONCLUSIONS

In this study, we synthesized the ZnO/GO composites of varying contents of ZnO in high quality using a facile one-step method. The composites own superior antibacterial properties against *E. coli* but exhibit low cytotoxicity. The antibacterial activity of the ZnO/GO composites is dependent on the content of zinc in the composites. It is mainly due to the synergistic effect of ZnO and GO: The possibility of bacteria contact to zinc was increased as ZnO NPs and released zinc ions from ZnO NPs were enriched on the GO sheets. The intimate contact of the *E. coli* cells and ZnO NPs on the GO sheets enhanced the permeability of the bacterial membrane and the local free zinc concentration around bacteria. In the future, the ZnO/GO composites containing formulations with high antibacterial ability and low toxicity may be utilized promisingly as disinfection agents in the surface coating on various substrates to effectively inhibit bacterial growth, propagation, and survival in medical devices.

EXPERIMENTAL SECTION

Preparation of the ZnO/GO Composites. GO used in this study was prepared and characterized following our previous work.[37] Before the synthesis of the composites, a GO suspension was centrifuged at 3000 rpm for 10 min (CR21GII, Hitachi, Japan) to remove any unexfoliated GO. $Zn(CH_3COO)_2{\cdot}2H_2O$ (0.55 g, ≥99%, Sinopharm Chemical Reagent Co., Ltd., China) was dissolved in 50.0 mL of absolute alcohol under vigorous stirring at 80 °C for 15 min, and then the mixture was cooled to 40 °C. After that, 0.20 g of $LiOH{\cdot}H_2O$ was dissolved in 30 mL of alcohol, and a GO suspension (2 mg mL^{-1}) was added to the above solution. The mixture was kept stirring for another 45 min. After cooling and the addition of 100 mL of *n*-hexane, the mixture was laid aside overnight at 4 °C. The obtained precipitate was collected by centrifugation and washed successively with ethanol and deionized water thoroughly to remove the solvent and impurity. After drying at 60 °C for 12 h in a vacuum oven, the ZnO/GO composite (mass ratio of ZnO/GO was 3:1) was obtained. We could synthesize ZnO/GO composites with different mass ratios of ZnO to GO by adjusting the quantity of Zn and GO. In this study, two composites were made: mass ratios of ZnO/GO of 3:1 (denoted as ZnO/GO-1) and 2:1 (denoted as ZnO/GO-2).

Characterization of the ZnO/GO Composites. The morphology of the composites was observed using a JEM-200CX microscope (JEOL, Japan) under an acceleration voltage of 120 kV for low-resolution TEM images. For a detailed investigation, we adopted a JEM-2010F microscope (JEOL, Japan) at an acceleration voltage of 200 kV for HRTEM images and an X-ray EDS for qualitative analysis of the composition of the composites. The specimens were prepared by dropping the sample dispersion onto a carbon-coated 300-mesh copper grid and dried under room temperature. The XRD patterns of the samples were recorded using a D/MAX-2500 diffractometer (Rigaku, Japan), equipped with a rotating anode and with a Cu Kα radiation source (λ = 1.54178 Å) at a scan speed of 2°/min with a step size of 0.02°. XPS of the ZnO/GO composites was measured using an AXIS Ultra instrument (Kratos, U.K.) at 293 K.

Antibacterial Test. *E. coli* was obtained from Peking University, China, and cultured with a Luria–Bertani (LB) culture medium (Sigma). Sterile LB broth and LB agar plates were prepared in deionized water according to the standard procedure.

The antibacterial activities of the ZnO/GO composites were evaluated qualitatively by the modified agar disk diffusion method that was recommended by the Clinical and Laboratory Standard Institute. Approximately 10^6 CFU mL^{-1} was inoculated on modified Sabouraud's agar plates. Filter papers with a diameter of 1.5 cm sucked with 10, 20, or 40 μL of a ZnO/GO-1 or ZnO/GO-2 nanocomposite suspension (100 μg mL^{-1}) were placed on the surface of seeded agar plate. After 16 h of incubation at 37 °C, the diameters of the inhibition zones were measured and optical images of the plates were taken.

The growth curves of *E. coli* after exposure to the ZnO/GO composites were plotted with the optical density (OD) versus time. *E. coli* (0.2 mL, ~10^8 CFU mL^{-1}) was inoculated in 10 mL of a fresh LB medium supplemented with 2.5, 5, 7.5, or 10 μg mL^{-1} of the ZnO/GO composites. The mixtures were then incubated in a rotary shaker at 150 rpm at 37 °C. The growth was monitored at an interval of 4 h for 24 h by measuring the increase of the OD at 600 nm using an UV–vis spectrophotometer (U-3010, Hitachi, Japan). All of the experiments were performed in triplicate, and the results are presented as mean ± standard deviation.

Morphology Investigation of *E. coli* after Exposure to the ZnO/GO Composites. To visualize the morphology of *E. coli* in detail after treatment with the composites, *E. coli* was cultured in a LB culture medium containing 10 μg mL^{-1} of ZnO/GO-1 or ZnO/GO-2 for 24 h. Upon centrifugation at 6000*g* (Hermle Z36HK, Germany) for 8 min, the bacteria were collected and washed with phosphate-buffered saline twice and then resuspended in double-distilled water. The suspension was filtered through a polycarbonate filter (Whatman nucleopore 0.2 μm) and was fixed in a glutaraldehyde solution (3 mL of 2.5% glutaraldehyde in 0.2 M sodium cacodylate/hydrochloric acid buffer, pH 7.5) at 4 °C for 2 h. The filters with the specimen were rinsed with the sodium cacodylate/hydrochloric acid buffer three times, followed by postfixing with a freshly prepared 1% osmium oxide solution for 1 h. Upon repeated rinses with double-distilled water, the specimen was dehydrated successively with graded ethanol solutions: 50% for 30 min, 75%, 85%, and 95% each for 10 min, and 100% for 10 min twice. Then the specimen was subjected to critical point drying to remove ethanol completely. Finally, it was mounted onto an aluminum stub, coated by gold sputter, and examined under a scanning electron microscope (JSM-6700F, Japan).

Release of Zinc from the ZnO/GO Composites. The release of zinc from the ZnO/GO composites in a LB culture medium was measured by inductively coupled plasma mass spectrometry (ICP-MS; ELAN DRC-e, PerkinElmer Co., USA). Briefly, the ZnO/GO composites were suspended in the LB culture medium (bacteria-free) with a final concentration of 0, 5, or 10 μg mL^{-1}. The mixtures were shaken in a rotary shaker at 150 rpm at 37 °C for 24 h. At certain time points (2, 4, 8, 12, 18, and 24 h), 500 μL of the mixtures was taken out and centrifuged (13500*g* × 10 min) to remove the

insoluble residues. The supernatants (400 μL) were collected and digested using HNO_3/H_2O_2 (1:1, v/v) at 100 °C for 15 min and diluted with 2% HNO_3 for ICP-MS measurements.

Cytotoxicity of the ZnO/GO Composites. In order to evaluate the cytotoxicity of GO and the ZnO/GO composites, HeLa cells were cultured with GO and the ZnO/GO composites, respectively. CCK-8 assay was used to determine the cell viability (Dojindo Molecular Technologies, Japan). Briefly, HeLa cells (~5×10^3 cells mL^{-1}) were plated in the 96-well plates (Corning, USA) and incubated for 24 h. ZnO/GO composites were introduced separately to cells with different final concentrations (5, 10, 20, 25, 30, and 50 μg mL^{-1}) in a culture medium. Cells cultured in the medium without adding any materials were taken as the control. After 24 h of incubation, the cells were washed with a D-Hanks buffer solution. A CCK-8 solution (150 μL) was added to each well and incubated for an additional 2 h at 37 °C. Then the samples in 96-well plates were centrifuged at 4500*g* for 15 min, and 100 μL of supernatant in each well was collected for the OD measurement at 450 nm on a microplate reader (Thermo, Varioskan Flash). The cell viability (percent of control) is expressed as the percentage of $(OD_{test} - OD_{blank})/(OD_{control} - OD_{blank})$, in which OD_{test} is the OD of the cells exposed to GO and ZnO/GO samples, $OD_{control}$ is the OD of the control sample, and OD_{blank} is the OD of the well samples without HeLa cells.

■ ASSOCIATED CONTENT

Supporting Information

Membrane integrity assay, adsorption of zinc ions on GO sheets, cytotoxicity of GO, and cytotoxicity of ZnO NPs. This material is available free of charge via the Internet at http://pubs.acs.org.

■ AUTHOR INFORMATION

Corresponding Author

*E-mail: hwang@shu.edu.cn. Tel: 86-21-66138026. Fax: 86-21-66135275.

Notes

The authors declare no competing financial interest.

■ ACKNOWLEDGMENTS

We thank the National Basic Research Program of China (973 Program; Grant 2011CB933402), the Chinese Natural Science Foundation (Grant 21071094), and Shanghai Leading Academic Disciplines (Grant S30109) for financial support.

■ REFERENCES

(1) Zhang, L.; Jiang, Y.; Ding, Y.; Povey, M.; York, D. Investigation into the Antibacterial Behaviour of Suspension of ZnO Nanoparticles (ZnO Nanofluids). *J. Nanopart. Res.* **2007**, *9*, 479−489.

(2) Kumar, K. M.; Mandal, B. K.; Naidu, E. A.; Sinha, M.; Kumar, K. S.; Reddy, P. S. Synthesis and Characterization of Flower Shaped Zinc Oxide Nanostructures and Its Antimicrobial Activity. *Spectrochim. Acta, Part A* **2013**, *104*, 171−174.

(3) Lipovsky, A.; Nitzan, Y.; Gedanken, A.; Lubart, R. Antifungal Activity of ZnO Nanoparticles—the Role of ROS Mediated Cell Injury. *Nanotechnology* **2011**, *22*, 105101.

(4) Vlad, S.; Tanase, C.; Macocinschi, D.; Ciobanu, C.; Balaes, T.; Filip, D.; Gostin, I. N.; Gradinaru, L. M. Antifungal Behaviour of Polyurethane Membranes with Zinc Oxide Nanoparticles. *Dig. J. Nanomater. Biostruct.* **2012**, *7*, 51−58.

(5) You, J.; Zhang, Y.; Hu, Z. Bacteria and Bacteriophage Inactivation by Silver and Zinc Oxide Nanoparticles. *Colloids Surf., B* **2011**, *85*, 161−167.

(6) FDA, 2011, http://ecfr.gpoaccess.gov/cgi/t/text/textidx?c=ecfr&sid=786bafc6f6343634fbf79fcdca7061e1&rgn=div5&view=text&node=21:3.0.1.1.13&idno=21#21:3.0.1.1.13.9.

(7) Kahru, A.; Dubourguier, H.-C.; Blinova, I.; Ivask, A.; Kasemets, K. Biotests and Biosensors for Ecotoxicology of Metal Oxide Nanoparticles: A Minireview. *Sensors* **2008**, *8*, 5153−5170.

(8) Brayner, R.; Ferrari-Iliou, R.; Brivois, N.; Djediat, S.; Benedetti, M.-F.; Fievet, F. Toxicological Impact Studies Based on *Escherichia coli* Bacteria in Ultrafine ZnO Nanoparticles Colloidal Medium. *Nano Lett.* **2006**, *6*, 866−870.

(9) Huang, Z.; Zheng, X.; Yan, D.; Yin, G.; Liao, X.; Kang, Y.; Yao, Y.; Huang, D.; Hao, B. Toxicological Effect of ZnO Nanoparticles Based on Bacteria. *Langmuir* **2008**, *24*, 4140−4144.

(10) Li, Y.; Zhang, W.; Niu, J.; Chen, Y. Mechanism of Photogenerated Reactive Oxygen Species and Correlation with the Antibacterial Properties of Engineered Metal−Oxide Nanoparticles. *ACS Nano* **2012**, *6*, 5164−5173.

(11) Deng, X.; Luan, Q.; Chen, W.; Wang, Y.; Wu, M.; Zhang, H.; Jiao, Z. Nanosized Zinc Oxide Particles Induce Neural Stem Cell Apoptosis. *Nanotechnology* **2009**, *20*, 115101.

(12) Lin, D.; Xing, B. Root Uptake and Phytotoxicity of ZnO Nanoparticles. *Environ. Sci. Technol.* **2008**, *42*, 5580−5585.

(13) Bai, W.; Zhang, Z.; Tian, W.; He, X.; Ma, Y.; Zhao, Y.; Chai, Z. Toxicity of Zinc Oxide Nanoparticles to Zebrafish Embryo: A Physicochemical Study of Toxicity Mechanism. *J. Nanopart. Res.* **2010**, *12*, 1645−1654.

(14) Williams, G.; Seger, B.; Kamat, P. V. TiO_2-Graphene Nanocomposites. UV-Assisted Photocatalytic Reduction of Graphene Oxide. *ACS Nano* **2008**, *2*, 1487−1491.

(15) Xu, C.; Wang, X.; Yang, L.; Wu, Y. Fabrication of a Graphene−Cuprous Oxide Composite. *J. Solid State Chem.* **2009**, *182*, 2486−2490.

(16) Zan, X.; Fang, Z.; Wu, J.; Xiao, F.; Huo, F.; Duan, H. Freestanding Graphene Paper Decorated with 2D-Assembly of Au@Pt Nanoparticles as Flexible Biosensors to Monitor Live Cell Secretion of Nitric Oxide. *Biosens. Bioelectron.* **2013**, *49*, 71−78.

(17) Zhang, L. L.; Zhao, X.; Stoller, M. D.; Zhu, Y.; Ji, H.; Murali, S.; Wu, Y.; Perales, S.; Clevenger, B.; Ruoff, R. S. Highly Conductive and Porous Activated Reduced Graphene Oxide Films for High-Power Supercapacitors. *Nano Lett.* **2012**, *12*, 1806−1812.

(18) Seema, H.; Christian, K. C.; Chandra, V.; Kim, K. S. Graphene−SnO_2 Composites for Highly Efficient Photocatalytic Degradation of Methylene Blue under Sunlight. *Nanotechnology* **2012**, *23*, 355705.

(19) Akhavan, O.; Ghaderi, E. Toxicity of Graphene and Graphene Oxide Nanowalls against Bacterial. *ACS Nano* **2010**, *4*, 5731−5736.

(20) Hu, W.; Peng, C.; Luo, W.; Lv, M.; Li, X.; Li, D.; Huang, Q.; Fan, C. Graphene-Based Antibacterial Paper. *ACS Nano* **2010**, *4*, 4317−4323.

(21) Liu, S.; Zeng, T. H.; Hofmann, M.; Burcombe, E.; Wei, J.; Jiang, R.; Kong, J.; Chen, Y. Antibacterial Activity of Graphite, Graphite Oxide, Graphene Oxide, and Reduced Graphene Oxide: Membrane and Oxidative Stress. *ACS Nano* **2011**, *5*, 6971−6980.

(22) Chang, Y.; Yang, S.-T.; Liu, J.-H.; Dong, E.; Wang, Y.-W.; Cao, A.; Liu, Y.; Wang, H. In Vitro Toxicity Evaluation of Graphene Oxide on A549 Cells. *Toxicol. Lett.* **2011**, *200*, 201−210.

(23) Zou, W.; Wu, J.; Sun, Y.; Wang, X. Depositing ZnO Nanoparticles onto Graphene in a Polyol System. *Mater. Chem. Phys.* **2011**, *125*, 617−620.

(24) Singh, G.; Choudhary, A.; Haranath, D.; Joshi, A. G.; Singh, N.; Singh, S.; Pasricha, R. ZnO Decorated Luminescent Graphene as a Potential Gas Sensor at Room Temperature. *Carbon* **2012**, *50*, 385−394.

(25) Lian, P.; Zhu, X.; Liang, S.; Li, Z.; Yang, W.; Wang, H. Large Reversible Capacity of High Quality Graphene Sheets as an Anode Material for Lithium-Ion Batteries. *Electrochim. Acta* **2010**, *55*, 3909−3914.

(26) Lang, J.; Han, Q.; Li, C.; Yang, J.; Li, X.; Yang, L.; Wang, D.; Zhai, H.; Gao, M.; Zhang, Y.; Liu, X.; Wei, M. Effect of Mn Doping on the Microstructure and Photoluminescence Properties of CBD Derived ZnO Nanorods. *Appl. Surf. Sci.* **2010**, *256*, 3365−3368.
(27) Zhang, W.; Cui, J.; Tao, C.; Wu, Y.; Li, Z.; Ma, L.; Wen, Y.; Li, G. A Strategy for Producing Pure Single-Layer Graphene Sheets Based on a Confined Self-Assembly Approach. *Angew. Chem., Int. Ed.* **2009**, *48*, 5864−5868.
(28) Raghupathi, K. R.; Koodali, R. T.; Manna, A. C. Size-Dependent Bacterial Growth Inhibition and Mechanism of Antibacterial Activity of Zinc Oxide Nanoparticles. *Langmuir* **2011**, *27*, 4020−4028.
(29) Li, M.; Zhu, L.; Lin, D. Toxicity of ZnO Nanoparticles to *Escherichia coli*: Mechanism and the Influence of Medium Components. *Environ. Sci. Technol.* **2011**, *45*, 1977−1983.
(30) Stoimenov, P. K.; Klinger, R. L.; Marchin, G. L.; Klabunde, K. J. Metal Oxide Nanoparticles as Bactericidal Agents. *Langmuir* **2002**, *18*, 6679−6686.
(31) Padmavathy, N.; Vijayaraghavan, R. Enhanced Bioactivity of ZnO Nanoparticles—An Antimicrobial Study. *Sci. Technol. Adv. Mater.* **2008**, *9*, 035004.
(32) Franklin, N. M.; Rogers, N. J.; Apte, S. C.; Batley, G. E.; Gadd, G. E.; Casey, P. S. Comparative Toxicity of Nanoparticulate ZnO, Bulk ZnO, and $ZnCl_2$ to a Freshwater Microalga (*Pseudokirchneriella subcapitata*): The Importance of Particle Solubility. *Environ. Sci. Technol.* **2007**, *41*, 8484−8490.
(33) Morones, J. R.; Elechiguerra, J. L.; Camacho, A.; Holt, K.; Kouri, J. B.; Ramirez, J. T.; Yacaman, M. J. The Bactericidal Effect of Silver Nanoparticles. *Nanotechnology* **2005**, *16*, 2346−2353.
(34) Yang, S.-T.; Liu, J.-H.; Wang, J.; Yuan, Y.; Cao, A.; Wang, H.; Liu, Y.; Zhao, Y. Cytotoxicity of Zinc Oxide Nanoparticles: Importance of Microenvironment. *J. Nanosci. Nanotechnol.* **2010**, *10*, 8638−8645.
(35) Buerki-Thurnherr, T.; Xiao, L.; Diener, L.; Arslan, O.; Hirsch, C.; Maeder-Althaus, X.; Grieder, K.; Wampfler, B.; Mathur, S.; Wick, P.; Krug, H. F. In Vitro Mechanistic Study towards a Better Understanding of ZnO Nanoparticle Toxicity. *Nanotoxicology* **2013**, *7*, 402−416.
(36) Shen, C.; James, S. A.; de Jonge, M. D.; Turney, T. W.; Wright, P. F. A.; Feltis, B. N. Relating Cytotoxicity, Zinc Ions, and Reactive Oxygen in ZnO Nanoparticle-Exposed Human Immune Cells. *Toxicol. Sci.* **2013**, *136*, 120−130.
(37) Cao, A.; Liu, Z.; Chu, S.; Wu, M.; Ye, Z.; Cai, Z.; Chang, Y.; Wang, S.; Gong, Q.; Liu, Y. A Facile One-Step Method to Produce Graphene−CdS Quantum Dot Nanocomposites as Promising Optoelectronic Materials. *Adv. Mater.* **2010**, *22*, 103−106.